

# Tet1 in Nucleus Accumbens Opposes Depression- and Anxiety-Like Behaviors

Jian Feng<sup>1,2</sup>, Catherine J Pena<sup>1</sup>, Immanuel Purushothaman<sup>1</sup>, Olivia Engmann<sup>1</sup>, Deena Walker<sup>1</sup>, Amber N Brown<sup>2</sup>, Orna Issler<sup>1</sup>, Marie Doyle<sup>1</sup>, Eileen Harrigan<sup>1</sup>, Ezekiel Mouzon<sup>1</sup>, Vincent Vialou<sup>1</sup>, Li Shen<sup>1</sup>, Meelad M Dawlaty<sup>3</sup>, Rudolf Jaenisch<sup>4,5</sup> and Eric J Nestler<sup>\*,1</sup>

<sup>1</sup>Fishberg Department of Neuroscience and Friedman Brain Institute, Icahn School of Medicine at Mount Sinai, New York, NY, USA; <sup>2</sup>Department of Biological Science, Florida State University, Tallahassee, FL, USA; <sup>3</sup>Department of Genetics and Gottesman Institute for Stem Cell and Regenerative Medicine Research, Albert Einstein College of Medicine, Bronx, NY, USA; <sup>4</sup>Whitehead Institute for Biomedical Research, Cambridge, MA, USA; <sup>5</sup>Department of Biology, Massachusetts Institute of Technology, Cambridge, MA, USA

Depression is a leading cause of disease burden, yet current therapies fully treat <50% of affected individuals. Increasing evidence implicates epigenetic mechanisms in depression and antidepressant action. Here we examined a possible role for the DNA dioxygenase, ten-eleven translocation protein 1 (TET1), in depression-related behavioral abnormalities. We applied chronic social defeat stress, an ethologically validated mouse model of depression-like behaviors, and examined *Tet1* expression changes in nucleus accumbens (NAc), a key brain reward region. We show decreased *Tet1* expression in NAc in stress-susceptible mice only. Surprisingly, selective knockout of *Tet1* in NAc neurons of adult mice produced antidepressant-like effects in several behavioral assays. To identify *Tet1* targets that mediate these actions, we performed RNAseq on NAc after conditional deletion of *Tet1* and found that immune-related genes are the most highly dysregulated. Moreover, many of these genes are also upregulated in the NAc of resilient mice after chronic social defeat stress. These findings reveal a novel role for TET1, an enzyme important for DNA hydroxymethylation, in the brain's reward circuitry in modulating stress responses in mice. We also identify a subset of genes that are regulated by TET1 in this circuitry. These findings provide new insight into the pathophysiology of depression, which can aid in future antidepressant drug discovery efforts.

*Neuropsychopharmacology* (2017) **42**, 1657–1669; doi:10.1038/npp.2017.6; published online 25 January 2017

## INTRODUCTION

Depression is a recurring and life-threatening illness that affects up to 20% of the population, yet <50% of patients respond fully to available treatments, which highlights the need for a better understanding of the syndrome and for improved treatments (Hyman, 2014; Krishnan and Nestler, 2008). Epigenetic mechanisms can encode environmental stimuli into behavioral adaptations throughout an individual's lifetime and have been implicated increasingly in several neuropsychiatric disorders, including depression (Akbarian, 2014; Bagot *et al*, 2014; Vialou *et al*, 2013). DNA methylation is a key epigenetic mechanism where methyl groups are covalently coupled to the C5 position of cytosine (5-methylcytosine (5mC)) (Jaenisch and Bird, 2003). The epigenetic modification of DNA provides an attractive regulatory mechanism underpinning the transcriptional alterations that contribute to the behavioral

abnormalities in brain disorders. However, the existence of a DNA methylation turnover pathway in the brain and its potential role in neural disorders have been elusive.

Ten-eleven translocation protein 1 (TET1) oxidizes 5mC into 5hydroxymethylcytosine (5hmC) (Kriaucionis and Heintz, 2009; Tahiliani *et al*, 2009). TET1, and the related family members TET2 and TET3, can also further oxidize 5hmC, eventually leading to unmethylated cytosine. This provides a mechanism by which 5mC oxidation mediates active DNA demethylation in the brain (Cheng *et al*, 2015; Guo *et al*, 2011). Although 5hmC is most enriched in the brain, the involvement of TETs and 5hmC in the regulation of adult brain function remains poorly understood. TETs and 5hmC have been shown to mediate active DNA demethylation in the hippocampus where they influence neural development, aging, neural plasticity, and learning and memory (Guo *et al*, 2011; Kaas *et al*, 2013; Li *et al*, 2014; Rudenko *et al*, 2013; Szulwach *et al*, 2011; Yu *et al*, 2015; Zhang *et al*, 2013). Recent evidence also suggests the involvement of TET/5hmC in neuropsychiatric disorders (Feng *et al*, 2015; Guidotti *et al*, 2013). For example, we found that TET1, acting in mouse nucleus accumbens (NAc)—a key reward region—negatively regulates cocaine reward behavior through widespread dynamic changes of 5hmC at responsive genes (Feng *et al*, 2015). In this study,

\*Correspondence: Dr EJ Nestler, Fishberg Department of Neuroscience and Friedman Brain Institute, Icahn School of Medicine at Mount Sinai, One Gustave L. Levy Place, Box 1065, New York, NY 10029-6574, USA, Tel: +1 212 659 5656, Fax: +1 212 659 1559. E-mail: eric.nestler@mssm.edu

Received 16 September 2016; revised 3 January 2017; accepted 5 January 2017; accepted article preview online 11 January 2017

we explored a potential role of TET1 in stress responses after chronic social defeat stress (CSDS), an ethologically validated model of depressive-like behaviors (Berton *et al*, 2006; Dias *et al*, 2014; Golden *et al*, 2011; Krishnan *et al*, 2007).

## MATERIALS AND METHODS

### Animals

For CSDS, 7–9-week-old male c57bl/6 mice from Jackson Laboratories were used. All mice were housed on a 12-h light/dark cycle with *ad libitum* access to food and water. CD1 retired breeder male mice were obtained from Charles River Laboratories. *Tet1*<sup>loxP/loxP</sup> mice (Dawlaty *et al*, 2011; Zhao *et al*, 2015) were backcrossed to a c57bl/6 background. Male homozygous offspring aged 7–9 weeks were used for viral manipulations and behavior assays. Biochemical assays were performed on bilateral 14 gauge punches of NAc. The Mount Sinai IACUC approved all experimental protocols.

### Chronic Social Defeat Stress

CSDS was performed as described (Dias *et al*, 2014; Golden *et al*, 2011). Briefly, an episode of social defeat involves placing a test intruder mouse into the home cage of a prescreened CD1 aggressor mouse, leading to an agonistic encounter. After 10 min, mice are separated by a perforated divider for the remainder of the 24-h period. This process is repeated daily for 10 days, each day with a novel CD1 mouse. In parallel, control animals are placed in pairs within an identical home cage setup, one control animal per side divided by a perforated divider, for the duration of the defeat sessions. After the last defeat session on day 10, all intruder and control mice are singly housed. Behavioral testing (eg, social interaction (SI)) was performed 24 h after the last defeat. A subgroup of defeated animals (termed ‘susceptible’) demonstrate marked social avoidance, which is associated with other behavioral and physiological changes reminiscent of depressive and anxiety symptoms. Social defeat also produces a subgroup of animals (termed ‘resilient’) that fails to develop social avoidance. Prior research has shown that susceptibility *vs* resilience is not related to the severity of aggression or injuries sustained (Krishnan *et al*, 2007). Bilateral 14 gauge NAc punches are collected 48 h after the last defeat unless otherwise noted.

### RNA Isolation and qPCR

RNA was extracted and purified using a Trizol-based protocol (Feng *et al*, 2015), as measured on a Nanodrop spectrophotometer. RNA was then reverse transcribed into cDNA with the iScript DNA Synthesis Kit (Bio-Rad). Real-time qPCR was performed with the  $\Delta\Delta C_t$  method to obtain relative fold change of expression as compared with control samples. *GAPDH* was utilized for normalization. Primers used in this study include:

*Anxa2*: 5'-CATCTGCTCACGAACCAACC-3', 5'-TCAGCTTTTCGGAAGTCTCCAG-3';

*Bst2*: 5'-CTGTAGAGACGGGTTGCGA-3', 5'-CTTCTTCCTCCAGGGACTCCTGA-3';

*Cd74*: 5'-TCCCAGAACCTGCAACTGGA-3', 5'-ATCAGCAAGGGAGTAGCCATC-3';

*Fgl2*: 5'-CCAGCCAAGAACACATGCAG-3', 5'-GGGTA ACTCTGTAGGCCCA-3';

*Gbp6*: 5'-ACTGAGAAGGAAGCTGGAGCAG-3', 5'-TCTCTCAGTTGCTGTATCTCTTTGT-3';

*H2-Aa*: 5'-GACCTCCCAGAGACCAGGAT-3', 5'-ACCA-TAGGTGCCTACGTGGT-3';

*H2-Ab1*: 5'-TTAGGAATGGGGACTGGACCT-3', 5'-TCTTGCTCCAGGCAGACTCA-3';

*H2-Eb1*: 5'-TCCGAAATGGAGACTGGACC-3', 5'-TGTTCTGTGCAGATGTGGATTG-3';

*Iigp1*: 5'-GGGGTGGGTCTCATGTGAAG-3', 5'-CCAAT-CACAGGCAAGTGTGC-3';

*Lcp2*: 5'-TGACTATGAGCCTCCACCCTC-3', 5'-TTTGTCTCAGTGGGGGCAC-3';

*Lyz2*: 5'-TGCTCAGGCCAAGGTCTATG-3', 5'-TGGTC TCCACGGTTGTAGTT-3';

*Ngb*: 5'-AGGACTGTCTCCTCTCCAG-3', 5'-CAAGC TGGTACAGTACTCCTC-3';

*Plscr1*: 5'-TGTGTAGCTGCTGTTCCGAC-3', 5'-ACATC-CAGGTCTAGCGGGAA-3';

*Serp1*: 5'-AGTGCCCATGATGAGTAGCG-3', 5'-CACGGGTACCACGATCACAA-3';

*Slc12a7*: 5'-CAACAAGCTGGCACTGGTCT-3', 5'-TCAAAGTTGCGATTTGCCAGC-3';

*Cxcl13*: 5'-ATTCAAGTTACGCCCCCTGG-3', 5'-TTGGCACGAGGATTCACACA-3';

*Cxcl9*: 5'-CGAGGCACGATCCACTACAA-3', 5'-CTTCA-CATTTGCCGAGTCCG-3';

*Igh1*: 5'-ACAGCACTTCCGTTTCAGTCA-3', 5'-GTGTA CACTGTGGAGCCTTC-3';

*Igkv6-23*: 5'-CATGGGCATCAAGATGGAGAC-3', 5'-CA-CATCCTGACTGGCCTTGC-3';

*Tet1*: 5'-GTCAGGGAGTCTCATGGAGAC-3', 5'-CCTGA-GAGCTCTCCCTTCC-3';

*Tet2*: 5'-GCAAGAGTCTCAGGGATGT-3', 5'-AGGTCGCACTCGTACCAAAC-3';

*Tet3*: 5'-CCAAGGCAAAGACCCTAACAA-3', 5'-AGCAAC TTCAGTGGCCAGAT-3';

*Tet1* exon 4: 5'-AGGTACACAAAAGAAAAAGGCC C-3', 5'-CCATGAGCTCCCTGACAGC-3';

*Tet1* exons 4 and 5 (Dawlaty *et al*, 2011): 5'-GTCAGG-GAGCTCATGGAGAC-3', 5'-CCTGAGAGCTCTTCCCTT CC-3' and

*GAPDH*: 5'-GGGTGTGAACCACGAGAAAT-3', 5'-GTC TTCTGGGTGGCAGTGAT-3'.

### Stereotaxic Surgeries

Surgery was performed under ketamine/xylazine anesthesia. AAV-Cre or AAV-GFP was infused bilaterally into the NAc at a rate of 0.1  $\mu$ l/min with the following coordinates: +1.6 mm A/P, +1.5 mm M/L,  $\pm$  4.4 mm D/V from Bregma. A total of 0.5  $\mu$ l/side was infused. All vectors were purchased from UNC Viral Core Facility. Behavioral assays were performed 4 weeks after viral injection. At the end of experiments, the brains of all animals were studied to confirm the accuracy of viral injections.

### Behavioral Tests

Mice subjected to CSDS or control conditions were examined in a battery of tests in the following order: SI,

sucrose preference, open field, and elevated-plus maze (EPM).

**Social interaction.** An SI test, performed as described (Golden et al, 2011), evaluates an experimental mouse's interaction with an empty cage vs a cage containing a novel CD1 target mouse. This test is used to distinguish susceptible mice, those that show decreased SI after CSDS, from resilient mice, those that avoid this abnormality (Berton et al, 2006; Krishnan et al, 2007). Briefly, an experimental mouse was allowed to explore an arena with an empty wire holding chamber for 150 s, immediately followed by 150 s of exploration in the same arena with a novel CD1 target mouse within the holding chamber. Ethovision software (Noldus) tracked animal movement from live video. Less time spent investigating the 'interaction zone' immediately surrounding the holding chamber containing the social target has been validated as depressive-like susceptible behavior.

**Sucrose preference.** Individually housed mice were first habituated to two bottles of water for 1 day, followed by 3 consecutive days with one bottle each of water and 1% sucrose (Krishnan et al, 2007). Consumption was measured by daily weighing, after which the two bottles were switched.

**Open field.** Each mouse is placed in the center of a chamber which they freely explore (Krishnan et al, 2007), with their activity and location measured by videotracking. Mice are allowed to freely explore the chamber, and they will typically spend a significantly greater amount of time

exploring the periphery of the arena, usually in contact with the walls, than the unprotected center area. Mice that spend significantly more time exploring the unprotected center area demonstrate anxiolytic-like baseline behavior.

**Elevated-plus maze.** Mice are placed in the center of an EPM, consisting of two interleaved open and closed arms, elevated 4 feet off the ground (Krishnan et al, 2007). Animals were placed in the center and time spent in open vs closed arms is measured using the Ethovision tracking software for 5 min. Measurement is of the time spent in the open arm or closed arm of maze.

## RNA Sequencing (RNAseq)

RNA integrity was confirmed by Bioanalyzer with RIN > 8.0. In all, 0.5 µg of total RNA was used for library construction using the Illumina Truseq mRNA Sample Prep Kit. All sequencing data were processed as previously described (Feng et al, 2014), with the voom package (Law et al, 2014) used for differential analyses with a cutoff of 30% change (> 1.3-fold or < 0.7-fold) and  $P$ -value < 0.05. Gene ontology analyses were carried out by DAVID (Huang da et al, 2009) with highest stringency settings. All RNAseq data are deposited into the Gene Expression Omnibus with accession number GSE76977.

## Statistical Analysis

Prism statistics package was used for data analyses. Two-tailed Student's  $t$ -test were used with statistical significance at

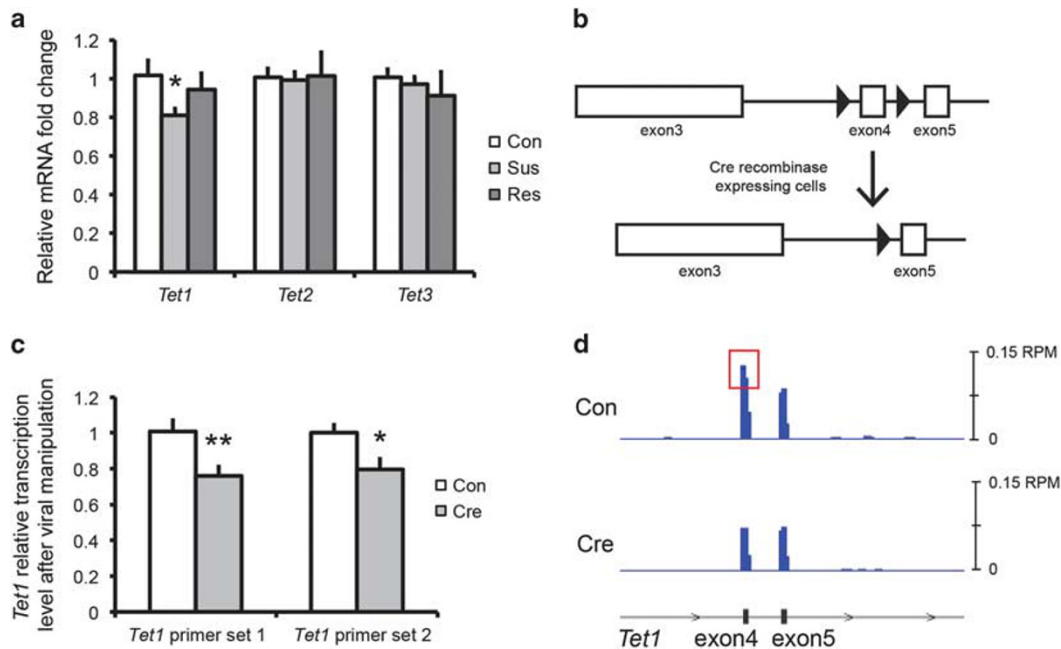


**Figure 1** Regulation of *Tet1* expression by CSDS. (a) *Tet1* mRNA levels are decreased in the NAc of susceptible mice 48 h after CSDS. (Con: control, Sus: susceptible, Res: resilient.  $N = 8$  for each group. Two-tailed  $t$ -test,  $*P = 0.025$ .) (b) Schematic of floxed *Tet1* locus (Dawlaty et al, 2011). Open boxes indicate exons of *Tet1* gene, black triangles represent loxP sites flanking exon 4, which is excised in the presence of Cre. (c) qPCR validation of *Tet1* decrease after AAV-Cre injection in NAc of floxed *Tet1* mice (Cre) as compared with AAV-GFP controls (Con). Two primer sets were used, which cover exon 4 alone (*Tet1* primer set 1) or both exons 4 and 5 (*Tet1* primer set 2) ( $N = 7$  for each group. Two-tailed  $t$ -test,  $*P = 0.011$ ,  $**P = 0.005$ ). (d) RNAseq read counts of *Tet1*. Schematic of relative position of exons 4 and 5 is shown on the bottom. Blue traces represent normalized read counts across these three exons in both control (Con) and Cre conditions under the same scale. Red box highlights differential reading of exon 4.

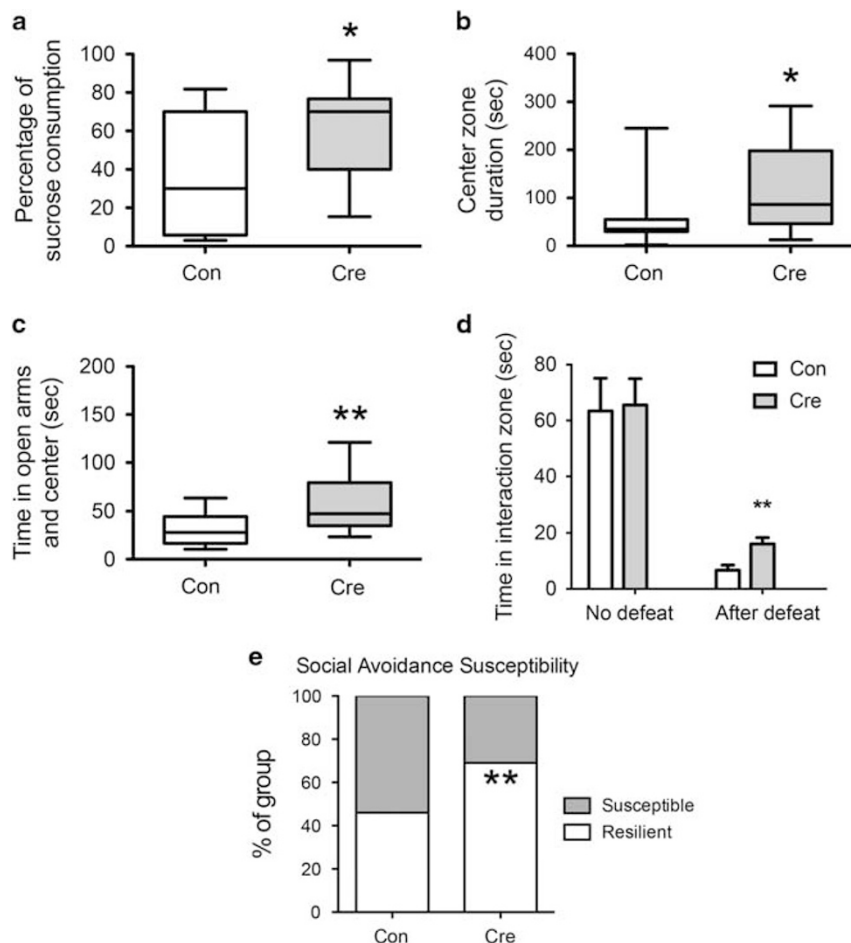


**Figure 2** *Tet1* KO from NAC induces antidepressant- and anxiolytic-like effects. (a) Floxed *Tet1* mice that received AAV-Cre in NAC exhibit increased sucrose preference ( $N = 15$  for each group. Two-tailed  $t$ -test,  $*P = 0.023$ ). (b) Cre mice also spent more time in the center zone in the open field test ( $N = 15$  for each group. Two-tailed  $t$ -test,  $*P = 0.024$ ) and (c) spent more time in the open arms in the EPM ( $N = 15$  for each group. Two-tailed  $t$ -test,  $**P = 0.008$ ). (d) Cre mice exhibited a partial rescue of social avoidance after CSDS ( $N = 13$  for each group. Two-tailed  $t$ -test,  $**P = 0.004$ ). (e) Cre mice demonstrated a greater percentage ( $**P = 0.001$  by a chi-squared test) of resilience (69% resilient vs 31% susceptible) than control mice (46% resilient vs 54% susceptible) 1 month after CSDS.

$P < 0.05$ . A chi-squared test was carried out to analyze the percentage of resilient mice after *Tet1* deletion.

## RESULTS

We first tested whether *Tet1* expression in NAC is affected by CSDS. In CSDS, ~65% of defeated animals (termed 'susceptible') demonstrate key behavioral abnormalities, such as social avoidance, with the remaining ~35% (termed 'resilient') not presenting these symptoms (Krishnan et al, 2007). We focused our studies on NAC based on its role in reward and motivation and its implication in the anhedonic aspects of depression (Russo and Nestler, 2013). Examining NAC tissue 48 h after the last defeat, we found a selective decrease in *Tet1* mRNA levels in the NAC of susceptible mice, but not in resilient mice, as compared with undefeated controls (Figure 1a). In contrast, neither *Tet2* nor *Tet3* expression was changed in either susceptible or resilient mice.

To study the functional consequences of *Tet1* suppression in NAC of susceptible mice, we injected AAV-Cre or AAV-

GFP bilaterally into NAC of *Tet1*<sup>loxP/loxP</sup> mice (Dawlaty et al, 2011), in which exon 4 is flanked by loxP sites (Figure 1b). By using two independent *Tet1* primer sets targeting exon 4, we found a small but significant decrease of *Tet1* transcripts in NAC 4 weeks after AAV-Cre injection (Figure 1c). The magnitude of decrease (~20%) is consistent with previous viral-mediated knockdowns (Dias et al, 2014) and likely reflects the fact that the AAV vectors used infected neurons only and that microdissections unavoidably contain non-infected tissue. The *Tet1* knockout (KO) was further confirmed by our RNAseq data (see below), where normalized read counts of *Tet1* exon 4 were similarly decreased in AAV-Cre- vs AAV-GFP-treated animals (Figure 1d).

We next studied mice with a *Tet1* KO in NAC in a battery of baseline behavioral assays. *Tet1* NAC-KO mice displayed increased preference of sucrose (Figure 2a). This result suggests that reduced *Tet1* expression in this brain region produces an antidepressant-like effect. *Tet1* NAC-KO mice also spent more time in the center zone in the open field test (Figure 2b), indicating a decrease in anxiety-like behavior. Further evidence for an anti-anxiety-like effect is increased

**Table 1** List of Differential Genes After *TetI* KO in Mouse NAc

Gene name	Fold change	P-value	Description
Mir5620	0.40943	0.00628	MicroRNA 5620
Gm23608	0.48335	0.04767	Predicted gene, 23608
Mir7026	0.52619	0.02050	MicroRNA 7026
Mir378b	0.55685	0.03154	MicroRNA 378b
Snord87	0.56160	0.00942	Small nucleolar RNA, C/D box 87
Gm25107	0.57947	0.03089	Predicted gene, 25107
Snord71	0.59732	0.01419	Small nucleolar RNA, C/D box 71
Gm22403	0.60480	0.04092	Predicted gene, 22403
Col19a1	0.63279	0.00461	Collagen, type XIX, alpha 1
Gm4134	0.65490	0.04335	Predicted gene 4134
Cdh24	0.66168	0.02585	Cadherin-like 24
Hs6st3	0.67161	0.04220	Heparan sulfate 6-O-sulfotransferase 3
Kcna2	0.69274	0.03252	Potassium voltage-gated channel, shaker-related subfamily, member 2
Clmp	0.69347	0.01709	CXADR-like membrane protein
Fank1	1.30177	0.01325	Fibronectin type 3 and ankyrin repeat domains 1
Tlr13	1.30561	0.02773	Toll-like receptor 13
Msn	1.30711	0.01301	Moesin
Cyp4v3	1.30756	0.00472	Cytochrome P450, family 4, subfamily v, polypeptide 3
Vcam1	1.30774	0.00199	Vascular cell adhesion molecule 1
Gm13091	1.30789	0.04192	Predicted gene 13091
Trim25	1.30794	0.03886	Tripartite motif-containing 25
Vav1	1.31024	0.04878	Vav 1 oncogene
Trim56	1.31163	0.01820	Tripartite motif-containing 56
Vamp8	1.31245	0.01777	Vesicle-associated membrane protein 8
Gm5617	1.31407	0.00419	Predicted gene 5617
Hist1h1c	1.31513	0.02795	Histone cluster 1, H1c
BC064078	1.31516	0.02451	cDNA sequence BC064078
Snora41	1.32091	0.03818	Small nucleolar RNA, H/ACA box 41
Fmo1	1.32591	0.01402	Flavin-containing monooxygenase 1
Casp8	1.32733	0.02303	Caspase 8
Ramp3	1.32976	0.03472	Receptor (calcitonin) activity-modifying protein 3
Crabp1	1.33142	0.03974	Cellular retinoic acid-binding protein 1
Plscr1	1.33552	0.00517	Phospholipid scramblase 1
H2-T22	1.33995	0.03738	Histocompatibility 2, T region locus 22
Srgn	1.34473	0.00888	Serglycin
Cnn2	1.34640	0.02238	Calponin 2
Lgals9	1.34649	0.00651	Lectin, galactose binding, soluble 9
Trim47	1.34755	0.00028	Tripartite motif-containing 47
Lyn	1.34809	0.01034	Yamaguchi sarcoma viral (v-yes-1) oncogene homolog
Tapbp	1.35200	0.00502	TAP-binding protein
Laptm5	1.35215	0.02647	Lysosomal-associated protein transmembrane 5
Tor3a	1.35320	0.00406	Torsin family 3, member A
Parp12	1.35466	0.00763	Poly (ADP-ribose) polymerase family, member 12
Akna	1.35491	0.04115	AT-hook transcription factor
Clic1	1.35517	0.01880	Chloride intracellular channel 1
Il4ra	1.35590	0.01444	Interleukin 4 receptor, alpha
Cryba4	1.36521	0.03467	Crystallin, beta A4
Fcgr3	1.36647	0.01738	Fc receptor, IgG, low affinity III
Ddx58	1.36871	0.01567	DEAD (Asp-Glu-Ala-Asp) box polypeptide 58
Ifit2	1.36909	0.00803	Interferon-induced protein with tetratricopeptide repeats 2
Hcls1	1.37127	0.03026	Hematopoietic cell specific Lyn substrate 1

Table 1 Continued

Gene name	Fold change	P-value	Description
Txnip	1.37744	0.02270	Thioredoxin interacting protein
Anxa2	1.37861	0.02668	Annexin A2
Slc12a7	1.38555	0.00396	Solute carrier family 12, member 7
Lcp1	1.39908	0.03649	Lymphocyte cytosolic protein 1
Al467606	1.39930	0.01706	Expressed sequence Al467606
Herc6	1.40607	0.01490	Hect domain and RLD 6
Gna15	1.40822	0.01684	Guanine nucleotide-binding protein, alpha 15
Pld4	1.40960	0.03691	Phospholipase D family, member 4
Hck	1.41077	0.02683	Hemopoietic cell kinase
Gm22540	1.41155	0.03746	Predicted gene, 22540
Aif1	1.41215	0.01643	Allograft inflammatory factor 1
Ifi27	1.41304	0.00945	Interferon, alpha-inducible protein 27
Prelp	1.41311	0.01697	Proline arginine-rich end leucine-rich repeat
Irf8	1.41402	0.03311	Interferon regulatory factor 8
Gpr84	1.41595	0.04632	G protein-coupled receptor 84
Lcp2	1.41757	0.00529	Lymphocyte cytosolic protein 2
Clec5a	1.41760	0.01871	C-type lectin domain family 5, member a
Atp6v1c2	1.42378	0.04810	ATPase, H <sup>+</sup> transporting, lysosomal VI subunit C2
Lck	1.42460	0.02505	Lymphocyte protein tyrosine kinase
Glpr2	1.42728	0.01827	GLI pathogenesis-related 2
Pim1	1.42978	0.02650	Proviral integration site 1
Trim12c	1.43162	0.01734	Tripartite motif-containing 12C
Trem2	1.43200	0.02741	Triggering receptor expressed on myeloid cells 2
Gsdmd	1.43433	0.01806	Gasdermin D
Myo1f	1.43552	0.04112	Myosin IF
Tifab	1.43699	0.03866	TRAF-interacting protein with forkhead-associated domain, family member B
Ctsh	1.43847	0.01280	Cathepsin H
Ifi30	1.44044	0.02082	Interferon gamma inducible protein 30
Clqc	1.44252	0.01818	Complement component 1, q subcomponent, C chain
Fermt3	1.44265	0.00815	Femitin family homolog 3 (Drosophila)
Fcgr1	1.44281	0.01467	Fc receptor, IgG, high affinity 1
Tnfrsf1b	1.44293	0.00807	Tumor necrosis factor receptor superfamily, member 1b
H2-DMb2	1.44303	0.04697	Histocompatibility 2, class II, locus Mb2
Il21r	1.45201	0.03540	Interleukin 21 receptor
Emr1	1.45279	0.02743	EGF-like module containing, mucin-like, hormone receptor-like sequence 1
Ptpn6	1.45486	0.01840	Protein tyrosine phosphatase, non-receptor type 6
Slc38a6	1.45598	0.00586	Solute carrier family 38, member 6
Cmtm7	1.45640	0.02481	CKLF-like MARVEL transmembrane domain containing 7
P2ry6	1.46150	0.01222	Pyrimidinergic receptor P2Y, G-protein coupled, 6
Mc3r	1.46158	0.04562	Melanocortin 3 receptor
Sox18	1.46202	0.02000	SRY (sex-determining region Y)-box 18
Cd86	1.46504	0.01271	CD86 antigen
Fyb	1.46712	0.03171	FYN-binding protein
AF251705	1.46771	0.02921	cDNA sequence AF251705
Clqb	1.47533	0.02403	Complement component 1, q subcomponent, beta polypeptide
Nfkb2	1.47575	0.00455	Nuclear factor of kappa light polypeptide gene enhancer in B cells 2, p49/p100
Tnfrsf13b	1.47639	0.01956	Tumor necrosis factor receptor superfamily, member 13b
S100a6	1.48034	0.02833	S100 calcium binding protein A6 (calcylin)
Gpsm3	1.48389	0.00650	G-protein signalling modulator 3 (AGS3-like, C. elegans)
Gm8034	1.48656	0.02555	Predicted gene 8034
Fcerlg	1.49547	0.02933	Fc receptor, IgE, high affinity I, gamma polypeptide

Table 1 Continued

Gene name	Fold change	P-value	Description
Itgb2	1.49570	0.02767	Integrin beta 2
Scama13	1.49960	0.01315	Small Cajal body-specific RNA 1
Ggta1	1.51058	0.03728	Glycoprotein galactosyltransferase alpha 1, 3
Sash3	1.51434	0.01935	SAM and SH3 domain containing 3
Tspo	1.51709	0.02372	Translocator protein
Rnf213	1.52106	0.01681	Ring finger protein 213
Ctsc	1.52112	0.00499	Cathepsin C
Pik3ap1	1.52152	0.01397	Phosphoinositide-3-kinase adaptor protein 1
Zc3hav1	1.52561	0.01009	Zinc finger CCCH type, antiviral 1
Cyba	1.52570	0.01098	Cytochrome b-245, alpha polypeptide
Gm27403	1.54968	0.01920	Predicted gene, 27403
Rarres2	1.55485	0.03157	Retinoic acid receptor responder (tazarotene induced) 2
Fcgr2b	1.56612	0.04813	Fc receptor, IgG, low affinity IIB
Snx20	1.57021	0.01682	Sorting nexin 20
Gm8995	1.57340	0.01718	Predicted gene 8995
I830012O16Rik	1.57424	0.00725	RIKEN cDNA I830012O16 gene
Mir760	1.57757	0.04202	MicroRNA 760
Was	1.59031	0.00811	Wiskott-Aldrich syndrome homolog (human)
Ifi35	1.59379	0.00251	Interferon-induced protein 35
Trim21	1.60197	0.00462	Tripartite motif-containing 21
Dtx3l	1.62101	0.00125	Deltex 3-like (Drosophila)
Cd84	1.62649	0.04608	CD84 antigen
Rac2	1.62903	0.01366	RAS-related C3 botulinum substrate 2
Lag3	1.62906	0.02312	Lymphocyte-activation gene 3
Isg15	1.62937	0.02034	ISG15 ubiquitin-like modifier
S100a4	1.63089	0.01624	S100 calcium-binding protein A4
Snord65	1.63262	0.02207	Small nucleolar RNA, C/D box 65
Slamf9	1.64065	0.01507	SLAM family member 9
Tap2	1.64229	0.00057	Transporter 2, ATP-binding cassette, sub-family B (MDR/TAP)
Clqa	1.64304	0.01171	Complement component 1, q subcomponent, alpha polypeptide
Ctss	1.64910	0.01101	Cathepsin S
Samd9l	1.65048	0.00293	Sterile alpha motif domain containing 9-like
Parp9	1.65148	0.00279	Poly (ADP-ribose) polymerase family, member 9
Capg	1.65831	0.03644	Capping protein (actin filament), gelsolin-like
Uba7	1.67736	0.00832	Ubiquitin-like modifier activating enzyme 7
H2-DMb1	1.68202	0.01181	Histocompatibility 2, class II, locus Mb1
Slc11a1	1.68809	0.01191	Solute carrier family 11 (proton-coupled divalent metal ion transporters), member 1
Gbp7	1.70194	0.00114	Guanylate-binding protein 7
Stat1	1.70605	0.00338	Signal transducer and activator of transcription 1
Icam1	1.71592	0.02338	Intercellular adhesion molecule 1
Lgals3bp	1.72057	0.00599	Lectin, galactoside-binding, soluble, 3 binding protein
Ifit3	1.73242	0.01078	Interferon-induced protein with tetratricopeptide repeats 3
Emp1	1.73254	0.02772	Epithelial membrane protein 1
Ifitm3	1.73492	0.00313	Interferon-induced transmembrane protein 3
Gbp9	1.75238	0.00527	Guanylate-binding protein 9
H2-M3	1.75247	0.00555	Histocompatibility 2, M region locus 3
Hist1h4h	1.76291	0.03228	Histone cluster 1, H4h
Cd48	1.77160	0.02161	CD48 antigen
AU020206	1.77649	0.02159	Expressed sequence AU020206
Serping1	1.78559	0.00447	Serine (or cysteine) peptidase inhibitor, clade G, member 1

Table I Continued

Gene name	Fold change	P-value	Description
Gbp3	1.78710	0.00194	Guanylate-binding protein 3
Irf1	1.78788	0.00241	Interferon regulatory factor 1
Rtp4	1.78924	0.00398	Receptor transporter protein 4
Lat	1.79364	0.03697	Linker for activation of T cells
Serpina3n	1.81634	0.04743	Serine (or cysteine) peptidase inhibitor, clade A, member 3N
Ifit1	1.82281	0.01432	Interferon-induced protein with tetratricopeptide repeats 1
Slfn2	1.82308	0.00158	Schlafen 2
Trim30a	1.83352	0.00506	Tripartite motif-containing 30A
Parp14	1.86180	0.00260	Poly (ADP-ribose) polymerase family, member 14
Vim	1.87536	0.00298	Vimentin
H2-T23	1.88738	0.00488	Histocompatibility 2, T region locus 23
Gbp5	1.92441	0.00052	Guanylate-binding protein 5
Dio3	1.93262	0.02592	Deiodinase, iodothyronine type III
Trim30d	1.94522	0.00196	Tripartite motif-containing 30D
Cxcl16	1.94934	0.00689	Chemokine (C-X-C motif) ligand 16
Cd52	1.98593	0.01242	CD52 antigen
Usp18	1.99617	0.02809	Ubiquitin-specific peptidase 18
Casp1	2.00205	0.00048	Caspase 1
Ighj4	2.01242	0.01101	Immunoglobulin heavy joining 4
Gm24991	2.01865	0.00612	Predicted gene, 24991
Irgm1	2.03356	0.00266	Immunity-related GTPase family M member 1
Fgl2	2.03545	0.00373	Fibrinogen-like protein 2
Cd274	2.04326	0.00267	CD274 antigen
AW112010	2.06189	0.00770	Expressed sequence AW112010
Oasl2	2.06654	0.01011	2'-5' Oligoadenylate synthetase-like 2
Psmb8	2.10971	0.00501	Proteasome (prosome, macropain) subunit, beta type 8 (large multifunctional peptidase 7)
Bst2	2.12044	0.00752	Bone marrow stromal cell antigen 2
Rn7sk	2.13533	0.01108	RNA, 7SK, nuclear
Ccl12	2.15282	0.00822	Chemokine (C-C motif) ligand 12
Gbp4	2.16135	0.00154	Guanylate-binding protein 4
B2m	2.16466	0.00266	Beta-2 microglobulin
Psmb9	2.23576	0.00354	Proteasome (prosome, macropain) subunit, beta type 9 (large multifunctional peptidase 2)
Lyz2	2.27020	0.00737	Lysozyme 2
C4b	2.34170	0.01555	Complement component 4B (Chido blood group)
Ngb	2.37059	0.02489	Neuroglobin
Tap1	2.42094	0.00164	Transporter 1, ATP-binding cassette, sub-family B (MDR/TAP)
Ly9	2.44460	0.00830	Lymphocyte antigen 9
Irgm2	2.48626	0.00267	Immunity-related GTPase family M member 2
H2-K1	2.51760	0.00204	Histocompatibility 2, K1, K region
H2-D1	2.52720	0.00257	Histocompatibility 2, D region locus 1
Gpnmb	2.57957	0.01409	Glycoprotein (transmembrane) nmb
Trac	2.62057	0.00322	T-cell receptor alpha constant
Gm7887	2.81379	0.04616	Predicted gene 7887
Lgals3	2.81867	0.00231	Lectin, galactose binding, soluble 3
Ltb	2.83335	0.00207	Lymphotoxin B
Gbp2	2.87958	0.00146	Guanylate binding protein 2
H2-Q4	3.09899	0.00212	Histocompatibility 2, Q region locus 4
Igtp	3.11780	0.00182	Interferon gamma induced GTPase
Fcgr4	3.13118	0.00271	Fc receptor, IgG, low affinity IV



Table 1 Continued

Gene name	Fold change	P-value	Description
Mzb1	3.17566	0.03032	Marginal zone B and B1 cell-specific protein 1
Gimap4	3.17867	0.00158	GTPase, IMAP family member 4
Cd79a	3.18865	0.02531	CD79A antigen (immunoglobulin-associated alpha)
Igkj2	3.23663	0.02824	Immunoglobulin kappa joining 2
Ifi47	3.25340	0.00025	Interferon gamma inducible protein 47
Gbp6	3.27693	0.00237	Guanylate-binding protein 6
Ighm	3.37635	0.02520	Immunoglobulin heavy constant mu
Igip1	3.46877	0.00067	Interferon inducible GTPase 1
Gimap3	3.58519	0.00327	GTPase, IMAP family member 3
H2-Q6	3.76649	0.00322	Histocompatibility 2, Q region locus 6
Igkj3	3.90029	0.02711	Immunoglobulin kappa joining 3
H2-Q7	4.34649	0.00250	Histocompatibility 2, Q region locus 7
Igkv6-15	4.49341	0.03924	Immunoglobulin kappa variable 6-15
Cxcl13	4.59804	0.01001	Chemokine (C-X-C motif) ligand 13
Igkj5	4.68025	0.01009	Immunoglobulin kappa joining 5
Ccl5	4.85390	0.00789	Chemokine (C-C motif) ligand 5
Cst7	4.93323	0.00432	Cystatin F (leukocystatin)
H2-Eb1	5.29583	0.00059	Histocompatibility 2, class II antigen E beta
H2-Ab1	5.41306	0.00060	Histocompatibility 2, class II antigen A, beta 1
Ighg2c	5.53995	0.03146	Immunoglobulin heavy constant gamma 2C
Iglv3	5.56594	0.01227	Immunoglobulin lambda variable 3
Igkj4	5.64314	0.00339	Immunoglobulin kappa joining 4
Cd74	5.76673	0.00082	CD74 antigen (invariant polypeptide of major histocompatibility complex, class II antigen associated)
H2-Aa	5.78797	0.00075	Histocompatibility 2, class II antigen A, alpha
Ighv1-55	6.28817	0.02826	Immunoglobulin heavy variable 1-55
Igi	6.44714	0.00556	Immunoglobulin joining chain
Cxcl10	6.45970	0.00402	Chemokine (C-X-C motif) ligand 10
Igkv1-110	7.35469	0.02618	Immunoglobulin kappa variable 1-110
Ighv1-81	7.50588	0.00728	Immunoglobulin heavy variable 1-81
Igkc	7.58698	0.01211	Immunoglobulin kappa constant
Ighv1-53	7.74927	0.04086	Immunoglobulin heavy variable 1-53
Igkv5-39	7.77156	0.03788	Immunoglobulin kappa variable 5-39
Ighv2-2	8.13349	0.02768	Immunoglobulin heavy variable 2-2
Igic2	8.16243	0.00338	Immunoglobulin lambda constant 2
Ighv1-34	8.24590	0.00685	Immunoglobulin heavy variable 1-34
Igkv12-41	8.24905	0.00599	Immunoglobulin kappa chain variable 12-41
Igha	8.29162	0.00492	Immunoglobulin heavy constant alpha
C3	8.54138	0.00232	Complement component 3
Ighv1-76	9.06576	0.01053	Immunoglobulin heavy variable 1-76
Igkv6-32	10.18662	0.02098	Immunoglobulin kappa variable 6-32
Ighv14-2	10.67261	0.00168	Immunoglobulin heavy variable 14-2
Ighg2b	10.76304	0.01809	Immunoglobulin heavy constant gamma 2B
Igkv17-121	11.15336	0.01178	Immunoglobulin kappa variable 17-121
Igkv5-48	11.30995	0.01648	Immunoglobulin kappa variable 5-48
Iglv1	12.10208	0.01184	Immunoglobulin lambda variable 1
Igkv16-104	12.65282	0.02023	Immunoglobulin kappa variable 16-104
Ighv1-26	13.14505	0.01634	Immunoglobulin heavy variable 1-26
Igkv10-96	13.75997	0.02022	Immunoglobulin kappa variable 10-96
Ighv1-18	14.15297	0.03178	Immunoglobulin heavy variable V1-18
Igkv4-59	14.79119	0.04511	Immunoglobulin kappa variable 4-59

Table 1 Continued

Gene name	Fold change	P-value	Description
Cxcl9	14.80531	0.00085	Chemokine (C-X-C motif) ligand 9
Ighv1-82	14.81065	0.00222	Immunoglobulin heavy variable 1-82
Igkv8-28	15.05572	0.00206	Immunoglobulin kappa variable 8-28
Ighv1-64	15.63836	0.00836	Immunoglobulin heavy variable 1-64
Ighv1-52	15.87288	0.02147	Immunoglobulin heavy variable 1-52
Igkv14-111	16.41352	0.01402	Immunoglobulin kappa variable 14-111
Igkv17-127	16.73881	0.00357	Immunoglobulin kappa variable 17-127
Igkv6-17	18.03311	0.00177	Immunoglobulin kappa variable 6-17
Ighv9-3	21.83215	0.00297	Immunoglobulin heavy variable V9-3
Igkv12-46	25.97771	0.01001	Immunoglobulin kappa variable 12-46
Igkv9-120	26.31750	0.00110	Immunoglobulin kappa chain variable 9-120
Igkv5-43	28.92911	0.00263	Immunoglobulin kappa chain variable 5-43
Igkv1-117	29.80211	0.00151	Immunoglobulin kappa variable 1-117
Igkv6-23	29.99634	0.00863	Immunoglobulin kappa variable 6-23
Ighg1	115.03142	0.00097	Immunoglobulin heavy constant gamma 1 (G1m marker)

time in the open arms of the EPM (Figure 2c). Of note, we did not detect significant changes in SI or forced swimming in non-stressed animals. Exposing *Tet1* NAc-KO and control mice to CSDS revealed that, although both groups showed social avoidance behavior, the *Tet1* NAc-KO mice displayed a partial reversal of this deficit (Figure 2d). *Tet1* NAc-KO also increased the percentage of resilient animals after CSDS (Figure 2e). This finding further supports an antidepressant-like action upon *Tet1* KO. Importantly, previous work has shown that overexpression of Cre in NAc of wild-type mice has no effect on any of these behavioral end points (Dias et al, 2014; Krishnan et al, 2007).

To understand the molecular underpinnings of these behavioral effects, we performed RNAseq to examine the gene expression changes in NAc upon a local *Tet1* KO without stress experience. The predominant effect of loss of *Tet1* is gene induction, with 252 genes upregulated in *Tet1* NAc-KO and only 14 genes downregulated (Table 1). Gene ontology analysis revealed that a large majority of the upregulated genes are concentrated in immune-related categories (Figure 3a). We then overlaid the upregulated and downregulated gene lists upon *Tet1* NAc-KO with an RNAseq data set of CSDS-induced gene expression changes in NAc 4 weeks after the last defeat (Bagot et al, 2016). This data set identified 140 upregulated and 86 downregulated genes in the resilient subgroup, and the upregulated genes showed a significant overlap with genes upregulated upon *Tet1* KO ( $N=15$  genes,  $P<1.586e-09$ , Figure 3b and d). In contrast, only four upregulated genes in *Tet1* KO were also induced in NAc of susceptible mice ( $P<0.022$ , Figure 3c).

To further confirm the potential molecular targets regulated by *Tet1* KO, we carried out quantitative PCR analyses on a set of 15 genes that demonstrate induction in NAc upon local *Tet1* KO based on our RNAseq data. Indeed, the majority ( $N=11$ ) of them were confirmed to have a significant increase after *Tet1* deletion (Figure 4), with most of the rest showing a trend toward increasing as well.

## DISCUSSION

We found a selective decrease in *Tet1* expression in NAc of mice that are susceptible to CSDS, an effect not seen in resilient mice. By use of viral-Cre-mediated deletion of *Tet1* in NAc neurons of adult mice, we showed that loss of *Tet1* in this brain region mediates antidepressant- and anxiolytic-like effects and that these behavioral actions are associated with the predominant induction of immune-related genes upon *Tet1* NAc-KO. The finding of a molecular change (*Tet1* suppression) in susceptible mice, but not in resilient mice that opposes the behavioral abnormalities associated with susceptibility, is surprising. It raises the interesting hypothesis that *Tet1* suppression in NAc is a homeostatic adaptation to counter susceptibility, which is not necessary in resilient mice that achieve resilience through other mechanisms. Indeed, the finding that a subset of genes induced in NAc upon *Tet1* NAc-KO are also induced in resilient (but not susceptible) mice supports this interpretation. The observation that *Tet1* NAc-KO only partially rescues the deleterious effects of CSDS supports the known involvement of many other genes in stress susceptibility (eg, Berton et al, 2006; Krishnan et al, 2007; Sun et al., 2015). In the future, it will be important to validate these findings in other stress models.

Increasing evidence supports a role for DNA methylation in mediating the effects of stress on the brain (Bagot et al, 2014). One well-studied example is glucocorticoid receptor (GR) gene methylation in response to early-life conditions (Turecki and Meaney, 2016). Different levels of maternal care control GR levels in the hippocampus of the offspring via DNA methylation changes, hence affecting hormonal and behavioral reactivity to stress. Foot shock stress reportedly alters DNA methyltransferase and methylation levels of candidate genes (Miller and Sweatt, 2007). We found that CSDS induces *Dnmt3a*, a *de novo* DNA methyltransferase, in NAc of susceptible mice and that *Dnmt3a* overexpression in this region increases depression-like behavior, while

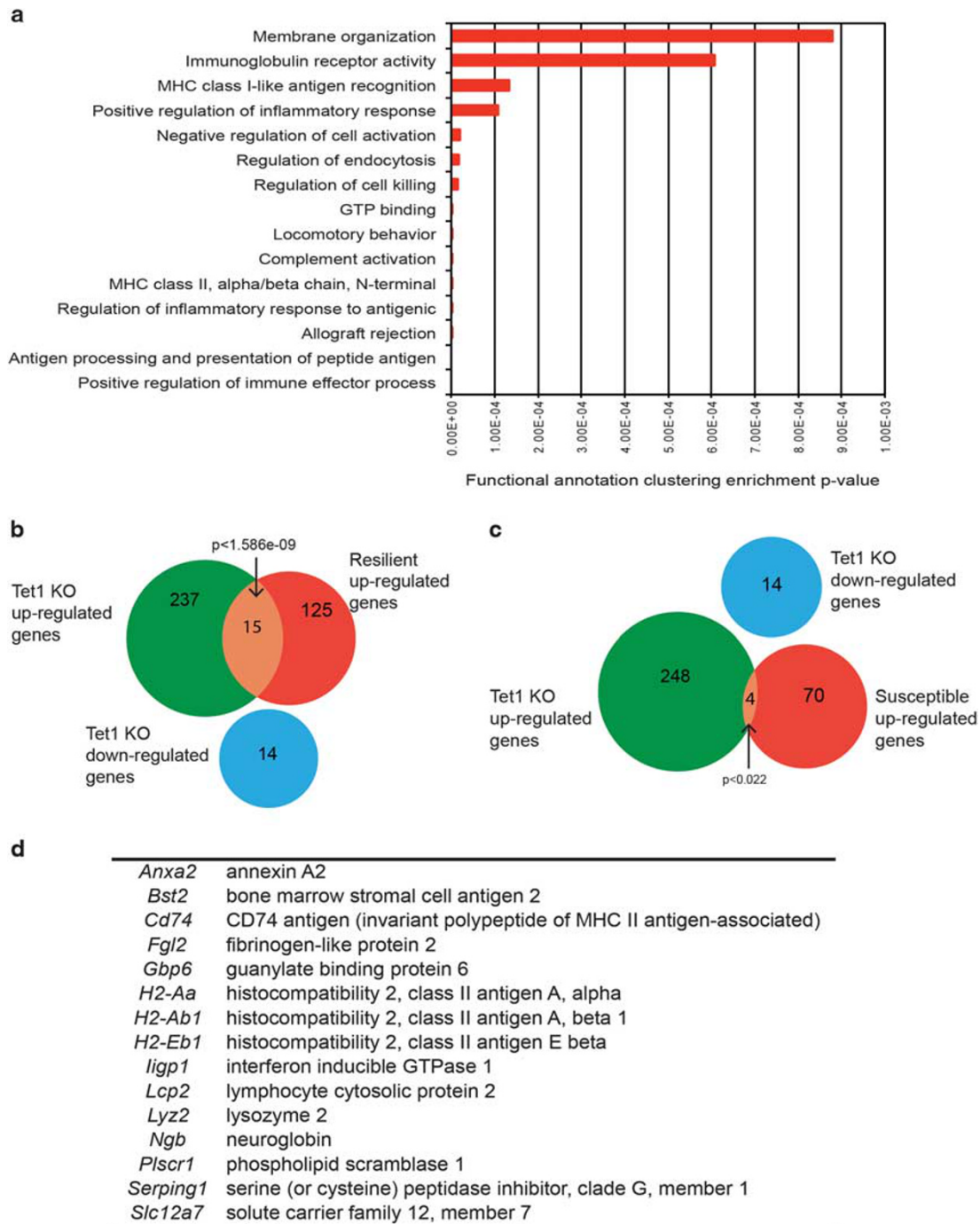


**Figure 3** Transcriptome analysis of *Tet1* KO from NAc. (a) Top 15 gene ontology enrichment terms and their corresponding *P*-values. (b) Venn diagrams of differential RNA gene lists reveals significant overlap ( $P < 1.586e-09$ ) between *Tet1* KO upregulated genes and genes upregulated in resilient mice 28 days after CSDS. Numbers of genes in each category are noted. (c) Venn diagrams of differential RNA gene lists reveal smaller overlap ( $P < 0.022$ ) between *Tet1* KO upregulated genes and genes upregulated in susceptible mice 28 days after CSDS. (d) List of overlapping genes in panel (b).

intra-NAc infusion of a DNMT inhibitor, RG108, exerts antidepressant-like effects (LaPlant *et al*, 2010).

The identification of TET enzymes and their products has reinforced the dynamic nature of DNA methylation. However, the role of TETs in brain function, particularly neuropsychiatric disorders, remains largely unknown. Through viral manipulations of TET1, Guo *et al* (2011) demonstrated that TET1 participates in neuronal activity-

induced, active DNA demethylation in the dentate gyrus of adult mice. Using similar approaches, TET1 overexpression was shown to impair memory formation (Kaas *et al*, 2013). As well, *Tet1* mutant mice exhibit abnormal adult hippocampal neurogenesis, long-term depression, and memory extinction (Rudenko *et al*, 2013; Zhang *et al*, 2013). Recently, by using viral overexpression and knockdown approaches, we found that TET1 in NAc negatively regulates cocaine

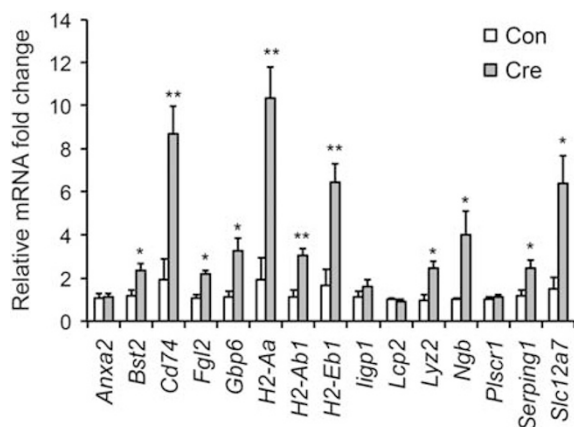


**Figure 4** qPCR validation of mRNA transcription change after *Tet1* KO. ( $N=5$  for each group. Two-tailed *t*-test, \* $P < 0.05$ , \*\* $P < 0.01$ .)

reward behavior (Feng *et al.*, 2015). Results of the present study extend these findings by revealing a previously unappreciated role for TET1 in NAc in stress responses.

Our RNAseq data show that the large majority of genes regulated by neuronal *Tet1* KO in NAc of stress-naïve mice are immune-related genes. Of note, previous studies have demonstrated a close relationship between alterations in DNA methylation and immune gene expression. For example, conditional KO of *Dnmts* in neuroblasts or postmitotic neurons yielded prominent dysregulation of immune gene clusters (Fan *et al.*, 2001; Feng *et al.*, 2010). It would now be important to directly study whether TET1 regulation of immune gene expression is associated with changes in 5mc or 5hmc at the affected loci. Our recent study directly linked loss of TET1 with increased 5hmc and induced gene expression at selective genes (Feng *et al.*, 2015). Although our present RNAseq data confirm the predominant upregulation of genes genome wide upon *Tet1* KO, further work is needed to better establish links among TET1, 5hmc, and gene expression. Of note, we did not detect the expression changes for several genes reported previously to be altered upon *Tet1* mutation or overexpression (Kaas *et al.*, 2013; Rudenko *et al.*, 2013). Such differences could be attributed to variations in brain region (NAc vs hippocampus), method of gene manipulation (AAV-Cre KO vs AAV overexpression or pan KO), or transcriptome profiling approach (RNAseq vs candidate gene analysis).

The significant overlap between genes upregulated in NAc upon *Tet1* KO or resilience after CSDS supports an important role of TET1 in stress-related disorders. The fact that most of the overlapping genes fall in immune categories provides further impetus for the importance of immune mechanisms in stress responses. Immune genes have long been implicated in neural development and plasticity and in learning and memory (Huh *et al.*, 2000). Neurons are known to express many genes traditionally characterized in the immune system (Neumann *et al.*, 1997). It is believed that certain immune molecules (eg, MHC I) mediate cellular immunity-like mechanisms in neuronal dendrite pruning and participate in neuropsychiatric diseases (Boulanger and Shatz, 2004; Stephan *et al.*, 2012). Additionally, recent evidence has identified depression-related disruptions in a

neuroimmune axis that interfaces between the immune and nervous systems. It is noteworthy that several recent studies have implicated inflammation as a possible cause for at least subtypes of depression and other stress-related disorders (Hodes *et al.*, 2015). Although targeting the neuroimmune axis for depression therapy is still at early stages, our data provide additional supporting evidence for this approach.

In summary, here we identified a novel role of DNA dioxygenase TET1 in stress responses, which offers new insight into both the pathophysiology of depression and the role played by this enzyme in neuronal adaptation. This highlights the importance of DNA epigenetics in the development of stress and other neuropsychiatric disorders and provides a foundation for future improvements in diagnosis and therapy.

## FUNDING AND DISCLOSURE

This work was supported by grants from the National Institute of Mental Health (to EJM), a NARSAD Young Investigator Award (to JF), and the Hope for Depression Research Foundation (HDRF). The authors declare no conflict of interest.

## REFERENCES

- Akbarian S (2014). Epigenetic mechanisms in schizophrenia. *Dialogues Clin Neurosci* **16**: 405–417.
- Bagot RC, Cates HM, Purushothaman I, Lorsch ZS, Walker DM, Wang J *et al.* (2016). Circuit-wide transcriptional profiling reveals brain region-specific gene networks regulating depression susceptibility. *Neuron* **90**: 969–983.
- Bagot RC, Labonte B, Pena CJ, Nestler EJ (2014). Epigenetic signaling in psychiatric disorders: stress and depression. *Dialogues Clin Neurosci* **16**: 281–295.
- Berton O, McClung CA, Dileone RJ, Krishnan V, Renthal W, Russo SJ *et al.* (2006). Essential role of BDNF in the mesolimbic dopamine pathway in social defeat stress. *Science* **311**: 864–868.
- Boulanger LM, Shatz CJ (2004). Immune signalling in neural development, synaptic plasticity and disease. *Nat Rev* **5**: 521–531.
- Cheng Y, Bernstein A, Chen D, Jin P (2015). 5-Hydroxymethylcytosine: a new player in brain disorders? *Exp Neurol* **268**: 3–9.
- Dawlaty MM, Ganz K, Powell BE, Hu YC, Markoulaki S, Cheng AW *et al.* (2011). Tet1 is dispensable for maintaining pluripotency and its loss is compatible with embryonic and postnatal development. *Cell Stem Cell* **9**: 166–175.
- Dias C, Feng J, Sun H, Shao NY, Mazei-Robison MS, Dames-Werno D *et al.* (2014). beta-catenin mediates stress resilience through Dicer1/microRNA regulation. *Nature* **516**: 51–55.
- Fan G, Beard C, Chen RZ, Csankovszki G, Sun Y, Siniaia M *et al.* (2001). DNA hypomethylation perturbs the function and survival of CNS neurons in postnatal animals. *J Neurosci* **21**: 788–797.
- Feng J, Shao N, Szulwach KE, Vialou V, Huynh J, Zhong C *et al.* (2015). Role of Tet1 and 5-hydroxymethylcytosine in cocaine action. *Nat Neurosci* **18**: 536–544.
- Feng J, Wilkinson M, Liu X, Purushothaman I, Ferguson D, Vialou V *et al.* (2014). Chronic cocaine-regulated epigenomic changes in mouse nucleus accumbens. *Genome Biol* **15**: R65.
- Feng J, Zhou Y, Campbell SL, Le T, Li E, Sweatt JD *et al.* (2010). Dnmt1 and Dnmt3a maintain DNA methylation and regulate synaptic function in adult forebrain neurons. *Nat Neurosci* **13**: 423–430.
- Golden SA, Covington HE 3rd, Berton O, Russo SJ (2011). A standardized protocol for repeated social defeat stress in mice. *Nat Protoc* **6**: 1183–1191.

- Guidotti A, Dong E, Gavin DP, Veldic M, Zhao W, Bhaumik DK et al (2013). DNA methylation/demethylation network expression in psychotic patients with a history of alcohol abuse. *Alcohol Clin Exp Res* 37: 417–424.
- Guo JU, Su Y, Zhong C, Ming GL, Song H (2011). Hydroxylation of 5-methylcytosine by TET1 promotes active DNA demethylation in the adult brain. *Cell* 145: 423–434.
- Hodes GE, Kana V, Menard C, Merad M, Russo SJ (2015). Neuroimmune mechanisms of depression. *Nat Neurosci* 18: 1386–1393.
- Huang, da W, Sherman BT, Lempicki RA (2009). Systematic and integrative analysis of large gene lists using DAVID bioinformatics resources. *Nat Protoc* 4: 44–57.
- Huh GS, Boulanger LM, Du H, Riquelme PA, Brotz TM, Shatz CJ (2000). Functional requirement for class I MHC in CNS development and plasticity. *Science* 290: 2155–2159.
- Hyman S (2014). Mental health: depression needs large human-genetics studies. *Nature* 515: 189–191.
- Jaenisch R, Bird A (2003). Epigenetic regulation of gene expression: how the genome integrates intrinsic and environmental signals. *Nat Genet* 33: 245–254.
- Kaas GA, Zhong C, Eason DE, Ross DL, Vachhani RV, Ming GL et al (2013). TET1 controls CNS 5-methylcytosine hydroxylation, active DNA demethylation, gene transcription, and memory formation. *Neuron* 79: 1086–1093.
- Kriaucionis S, Heintz N (2009). The nuclear DNA base 5-hydroxymethylcytosine is present in Purkinje neurons and the brain. *Science* 324: 929–930.
- Krishnan V, Han MH, Graham DL, Berton O, Renthal W, Russo SJ et al (2007). Molecular adaptations underlying susceptibility and resistance to social defeat in brain reward regions. *Cell* 131: 391–404.
- Krishnan V, Nestler EJ (2008). The molecular neurobiology of depression. *Nature* 455: 894–902.
- LaPlant Q, Vialou V, Covington HE 3rd, Dumitriu D, Feng J, Warren BL et al (2010). Dnmt3a regulates emotional behavior and spine plasticity in the nucleus accumbens. *Nat Neurosci* 13: 1137–1143.
- Law CW, Chen Y, Shi W, Smyth GK (2014). voom: Precision weights unlock linear model analysis tools for RNA-seq read counts. *Genome Biol* 15: R29.
- Li X, Wei W, Zhao QY, Widagdo J, Baker-Andresen D, Flavell CR et al (2014). Neocortical Tet3-mediated accumulation of 5-hydroxymethylcytosine promotes rapid behavioral adaptation. *Proc Natl Acad Sci USA* 111: 7120–7125.
- Miller CA, Sweatt JD (2007). Covalent modification of DNA regulates memory formation. *Neuron* 53: 857–869.
- Neumann H, Schmidt H, Cavalie A, Jenne D, Wekerle H (1997). Major histocompatibility complex (MHC) class I gene expression in single neurons of the central nervous system: differential regulation by interferon (IFN)-gamma and tumor necrosis factor (TNF)-alpha. *J Exp Med* 185: 305–316.
- Rudenko A, Dawlaty MM, Seo J, Cheng AW, Meng J, Le T et al (2013). Tet1 is critical for neuronal activity-regulated gene expression and memory extinction. *Neuron* 79: 1109–1122.
- Russo SJ, Nestler EJ (2013). The brain reward circuitry in mood disorders. *Nat Rev* 14: 609–625.
- Stephan AH, Barres BA, Stevens B (2012). The complement system: an unexpected role in synaptic pruning during development and disease. *Annu Rev Neurosci* 35: 369–389.
- Sun H, Damez-Werno DM, Scobie KN, Shao NY, Dias C, Rabkin J et al (2015). ACF chromatin-remodeling complex mediates stress-induced depressive-like behavior. *Nat Med* 21: 1146–1153.
- Szulwach KE, Li X, Li Y, Song CX, Wu H, Dai Q et al (2011). 5-hmC-mediated epigenetic dynamics during postnatal neurodevelopment and aging. *Nat Neurosci* 14: 1607–1616.
- Tahiliani M, Koh KP, Shen Y, Pastor WA, Bandukwala H, Brudno Y et al (2009). Conversion of 5-methylcytosine to 5-hydroxymethylcytosine in mammalian DNA by MLL partner TET1. *Science* 324: 930–935.
- Turecki G, Meaney MJ (2016). Effects of the social environment and stress on glucocorticoid receptor gene methylation: a systematic review. *Biol Psychiatry* 79: 87–96.
- Vialou V, Feng J, Robison AJ, Nestler EJ (2013). Epigenetic mechanisms of depression and antidepressant action. *Annu Rev Pharmacol Toxicol* 53: 59–87.
- Yu H, Su Y, Shin J, Zhong C, Guo JU, Weng YL et al (2015). Tet3 regulates synaptic transmission and homeostatic plasticity via DNA oxidation and repair. *Nat Neurosci* 18: 836–843.
- Zhang RR, Cui QY, Murai K, Lim YC, Smith ZD, Jin S et al (2013). Tet1 regulates adult hippocampal neurogenesis and cognition. *Cell Stem Cell* 13: 237–245.
- Zhao Z, Chen L, Dawlaty MM, Pan F, Weeks O, Zhou Y et al (2015). Combined loss of Tet1 and Tet2 promotes B cell, but not myeloid malignancies, in mice. *Cell Rep* 13: 1692–1704.